MATHEMATICAL BIOSCIENCES
AND ENGINEERING
Volume **10**, Number **2**, April **2013**

doi:10.3934/mbe.2013.10.399

pp. **399–424**

COMPETITION OF MOTILE AND IMMOTILE BACTERIAL STRAINS IN A PETRI DISH

Silogini Thanarajah and Hao Wang

Department of Mathematical and Statistical Sciences, University of Alberta
Edmonton, Alberta, T6G 2G1, Canada

(Communicated by Yuan Lou)

Abstract. Bacterial competition is an important component in many practical applications such as plant roots colonization and medicine (especially in dental plaque). Bacterial motility has two types of mechanisms — directed movement (chemotaxis) and undirected movement. We study undirected bacterial movement mathematically and numerically which is rarely considered in literature. To study bacterial competition in a petri dish, we modify and extend the model used in Wei et al. (2011) to obtain a group of more general and realistic PDE models. We explicitly consider the nutrients and incorporate two bacterial strains characterized by motility. We use different nutrient media such as agar and liquid in the theoretical framework to discuss the results of competition. The consistency of our numerical simulations and experimental data suggest the importance of modeling undirected motility in bacteria. In agar the motile strain has a higher total density than the immotile strain, while in liquid both strains have similar total densities. Furthermore, we find that in agar as bacterial motility increases, the extinction time of the motile bacteria decreases without competition but increases in competition. In addition, we show the existence of traveling-wave solutions mathematically and numerically.

1. **Introduction.** Bacteria are a major domain of single-celled microorganisms and play an essential role in the maintenance of energy and nutrients throughout our world. In most natural environments, bacteria compete with neighbors for space and nutrients [7]. Bacteria can be beneficial or harmful to us when they grow and reproduce. Bacterial strains are recognized by their appearance, the types of nutrients they can grow on, the types of substances they produce, etc..

Motile bacteria can move using flagella or glide over surfaces by movement mechanisms [30, 25]. The majority of bacteria can display self-propelled movement (motility) under suitable conditions [4, 8]. The most studied bacterial cell movements are recognized as direct (runs) and undirect (tumbles). When a bacterial cell moves towards a chemical (attractants) or directly away from a chemical (repellents), this process is called chemotaxis [22, 10, 30]. In some cases, chemotaxis climbs a chemical gradient because of the chemical distribution. On the other hand, bacteria with flagella and other mechanisms can move in random directions [28]. In the absence of chemotaxis, a species with a small enough random motility can grow to a larger population size than a second population with a greater growth rate.

2010 *Mathematics Subject Classification.* Primary: 92B05, 35Kxx, 35C07; Secondary: 92D25, 92D40, 35B35.

Key words and phrases. Motility, competition, diffusion, traveling-wave solution, extinction time, partial differential equation.

[15]. Many existing theoretical studies assume that bacteria have to move in the direction of nutrients [19, 18, 5, 6]. However, there have been a few papers that do not assume directional movement of motile bacteria [28, 14, 24]. The recent PNAS paper [28] suggests that undirected movement has been overlooked in literature. In most cases, flagella evolved after motility was in place [28]. Some types of bacteria, such as *E.coli*, move in a random direction when the coordinated motion of the flagella stops because the flagella has turned in the opposite direction [31, 32]. In this theoretical work, we assume that bacteria have undirected movement to reach nutrient. Recent studies show that motility provides a selective compensation in the unshaken cultures because motile cells could move actively to acquire growth-limiting nutrients [29]. In addition, undirected motility can be more important in resource-homogeneous environments or when the chemicals are not chemotactic stimuli.

A few studies have been done to discuss the role of random motility on bacterial competition. Lauffenburger et al. (1981) developed a reaction diffusion model for a bacterial population to study the effects of chemical diffusion and cell random motility in a finite one-dimensional, non-mixed region. In this system, the effect of random motility of the population depended on the relative magnitude of the diffusion coefficient compared to the growth rate. Lauffenburger et al (1983) extended their earlier work by including chemotaxis. They studied a competitive growth of two randomly motile populations in a finite non-mixed region. This system yielded up to three possible steady states. Later, Wei et al. (2011) developed a reaction diffusion model to study the existence of undirected motility in bacteria. Their work was motivated by lab experimental results testing their theoretical predictions. They used different nutrient media such as agar and liquid in their experiments. Their study suggested that chemotaxis evolved in bacteria that were already capable of self-propulsion in random directions. Our work is motivated by the experimental observations of Wei et al. (2011). We extend a Wei et al. (2011) model by including mortality rates to study competitive results of motile and immotile bacterial strains in a finite one and two-dimensional, non-mixed region. Our motivation is to test whether the model is suitable for elucidating bacterial random motility by comparing numerical results with the experimental results of Wei et al. (2011). Beyond this comparison, we additionally obtain extinction time (for long term competition) and traveling-wave solutions (for invasion).

The focus of our work is to use bacteria as a model organism to study the competition of two strains in a petri dish. The assumption for our model is that there are two kinds of bacterial strains: the motile strain that moves quickly and the immotile strain that moves very slowly [27, 17]. Nutrient media vary from agar to liquid by changing the nutrient diffusion rate. We apply this theoretical framework to verify the study of undirected motility in bacterial movement and discuss the role of motility and nutrient medium types in determining bacterial competition. Our simulation results exhibit that the role of undirected motility is preferred by bacteria in the agar case because it increases the chance of getting nutrients. We run one-dimensional spatial simulations to compute extinction times, traveling-wave solutions and the total densities of both bacterial strains, and we run two-dimensional spatial simulations to exhibit pattern formation. We present rigorous mathematical analysis of steady states, asymptotical behaviors of solutions, and traveling-wave solutions. Proofs of mathematical results are placed in the

Appendix. Our PDE model can elucidate and validate petri dish experimental results [28] under homogeneous nutrient distribution.

2. **Mathematical model.** In literature, many papers have considered the directed and undirected movements of bacteria [28, 24, 14, 19, 18]. We extend the existing model [28] to incorporate mortality rates and general diffusion terms (especially in polar coordinates for the disk shape of petri dish). With these new components in the theoretical framework, we can discuss the long term behavior of solutions such as steady states, asymptotic behavior, and extinction time.

Agar is a gelatinous substance made from red algae. It is used as a solid culture media for bacteria and other microorganisms. We consider the reaction-diffusion competition model for agar media as follows:

$$\begin{aligned} \frac{\partial B_i}{\partial t} &= D_i \Delta B_i + [h_i(N) - \delta_i] B_i, \\ \frac{\partial N}{\partial t} &= -\sum_i \frac{1}{\gamma_i} h_i(N) B_i, \end{aligned}$$

where $\Delta = \frac{\partial^2}{\partial x^2}$, $i = 1, 2, \cdots, m$, $\vec{x} \in \Omega$ and the consumption function $h_i(N)$ satisfies the conditions $h_i(0) = 0$, $h_i'(t) > 0$, and $h_i''(t) \leq 0$, for example, $h_i(N) = \alpha_i N/(k_i + N)$ or $h_i(N) = \alpha_i N$. Here m is a positive integer representing the number of competing bacterial species. The model has initial conditions: $N(0, \vec{x}) = N_0$ for $\vec{x} \in \Omega$, $B_i(0, \vec{x}) = B_0$ (small and supported in a small disk) for each i on Ω, and Neumann boundary conditions (zero flux): $\nabla B \cdot \vec{n} = 0$ on $\partial\Omega$, where $\vec{n}$ is a outward normal vector to the boundary $\partial\Omega$.

Here $B_i(x, t)$, $N(x, t)$ represent the density of ith bacterial strain and the density of nutrients respectively, with diffusion coefficients D_i. Ω is a bounded domain in $[0, L] \subseteq \mathbb{R}$ or $\mathbb{R}^2$, δ_i is a mortality rate, and γ_i is the yield constant ($1/\gamma_i$ units of nutrient are consumed in producing one unit of bacterial biomass). All parameters are nonnegative constants.

In the next few sections, we establish the case of a single bacterial strain (no competition) and the case of two competing bacterial strains (motile versus immotile). The liquid media case will be introduced for a comparison with the agar media case. mathematical results will only be provided for agar models, which are our main focus.

3. **Single bacterial species in a petri dish.** First, we consider the model for a single bacterial strain in one-dimensional and two-dimensional spaces. We perform rigorous mathematical analysis including uniform and non-uniform steady states, traveling-wave solutions, and non-extinction of nutrients. Finally, we compute the extinction time and determine its dependence on key parameters.

3.1. **Mathematical analysis.** The single species model is provided by

$$\begin{aligned} &\frac{\partial B}{\partial t} = D\Delta B + (h(N) - \delta)B, \\ &\frac{\partial N}{\partial t} = -\frac{1}{\gamma} h(N) B, \qquad \text{where } \gamma < 1 \text{ is the yield constant,} \end{aligned} \tag{1}$$

the initial conditions are:

$$\begin{aligned} B(x, 0) &= B_0 \quad \text{(small and supported in a small disk)}, \\ N(x, 0) &= N_0, \end{aligned}$$

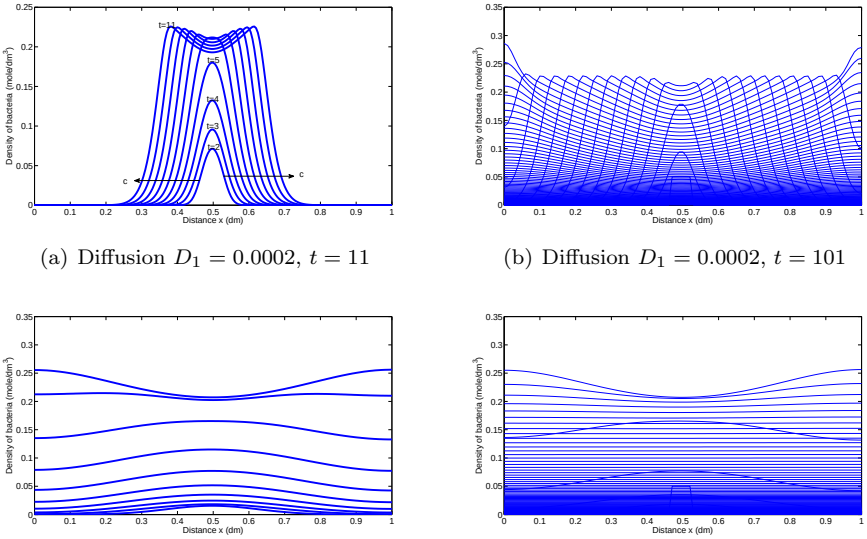

(a) Diffusion $D_1 = 0.0002$, $t = 11$

(b) Diffusion $D_1 = 0.0002$, $t = 101$

(c) Diffusion $D_1 = 0.008$, $t = 11$

(d) Diffusion $D_1 = 0.008$, $t = 101$

FIGURE 1. Numerical simulations show the existence of traveling-wave solutions for the system (1) with $D_1 = 0.0002$ or $D_1 = 0.008$. We run simulations for the shorter time ($t = 11$) and the longer time ($t = 101$). Different curves represent different times. The details of panels (b), (c), (d) are similar to panel (a). The parameter c is the traveling wave speed. If we make a cross-section, the distances between any two consecutive curves are the same.

the boundary conditions are:

$$\frac{\partial B}{\partial x}(0,t) = \frac{\partial B}{\partial x}(L,t) = 0 \quad \text{on} \quad \partial\Omega.$$

Our first theorem states equilibrium results for one-dimensional and two-dimensional (disk case) spaces.

Theorem 3.1. *The system of equations (1) with Neumann boundary conditions admits infinitely many steady states* $(0, \overline{N})$ *where* $\overline{N} = \overline{N}(\vec{x}) \geq 0$, $\vec{x}$ *is the vector of spatial variable(s). In addition, we show that for equilibrium solutions, if* $N = 0$ *then* $B = 0$.

We study traveling-wave solutions for a system of two equations representing a single bacterial strain and nutrient. For simplicity, we only discuss one-dimensional space case. The effect of growth and random movement in a homogeneous environment on the bacterial population, which generates a colony, leads to traveling wave. Now we discuss the existence of traveling-wave solutions and their minimum traveling speed.

We are looking for traveling-wave solutions of the reaction-diffusion model (1) in a homogeneous nutrient environment. There exists some solution $(B(t,x),N(t,x))$ which satisfies the following conditions:

(i) $B(t,x)$ tends to a solitary wave such that [9]

$$B_x \to 0 \qquad \text{as} \qquad x \to \pm\infty,$$
$$B \to 0 \qquad \text{as} \qquad x \to \pm\infty,$$

and (ii) $N(t,x)$ tends to a transition wave such that [9]

$$N \to 1 \qquad \text{as} \qquad x \to +\infty,$$
$$N \to n(-\infty)(=n) \qquad \text{as} \qquad x \to -\infty.$$

Note that $n(-\infty) = n$ is an unknown constant. Based on the above conditions, we have the following theorem:

Theorem 3.2. *The model (1) admits traveling-wave solutions if* $c \geq c_{min} = c^* \equiv 2(\frac{D\sigma(1)}{\gamma})^{1/2}$, *where* $\sigma(\bar{N}_s) = -h(\bar{N}_s)\phi'(\bar{N}_s)$, $\phi(\bar{N}) = \gamma\left(1 - \bar{N} - \delta\int_{\bar{N}}^{1}\frac{d\bar{n}}{h(\bar{n})}\right)$. *The parameter c is the traveling wave speed.*

Biologically, the bacterial population creates a symbiosis with nutrient source causing the formation of traveling wave. In our case, the bacterial population invades an area of the petri dish where the nutrient has already stabilized.

In Fig.1, we numerically show traveling-wave solutions for different diffusion rates of motile bacteria with long and short time periods. As the motility of motile bacteria increases, traveling waves propagate faster, thus it takes less time for motile bacteria to occupy the non-centered region of the petri dish.

It follows from second equation of (1) that for fixed $\vec{x} \in \Omega$, the nutrient density $N(\vec{x},t)$ is monotone decreasing in t with the limit $N_\infty(\vec{x})$. Based on these results, we have the following theorem:

Theorem 3.3. *When the consumption function* $h(N)$ *takes natural forms* αN *or* $\frac{\alpha N}{k+N}$, *then nutrient never gets completely consumed at any position. More precisely, if* $N(\vec{x},0) > 0$, *then* $N_\infty(\vec{x}) = \lim_{t\to\infty} N(\vec{x},t) > 0$.

3.2. **Liquid case.** Chemically defined basal liquid media, simply made by nutrient soup, are used to provide nutrients for cell growth in lab. Our model was developed to study competition in agar media but can be easily modified for liquid media. We use the following liquid model to compare with the agar case because the experiment was performed to test both cases. The single species model for liquid media is provided by

$$\begin{aligned}\frac{\partial B}{\partial t} &= D\Delta B + (h(N) - \delta)B,\\ \frac{\partial N}{\partial t} &= D_3\Delta N - \frac{1}{\gamma}h(N)B, \qquad \text{where } \gamma < 1 \text{ is the yield constant,}\end{aligned}$$

the initial conditions are:

$$\begin{aligned}B(x,0) &= B_0 \quad \text{(small and supported in a small disk)},\\ N(x,0) &= N_0,\end{aligned}$$

the boundary conditions are:

$$\frac{\partial B}{\partial x}(0,t) = \frac{\partial B}{\partial x}(L,t) = 0 \quad \text{on} \quad \partial\Omega.$$

The two species model for liquid media will be presented in section 4.3.

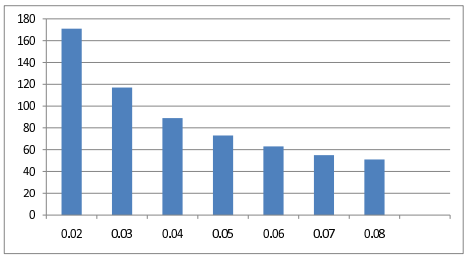

(a) T_0 vs δ

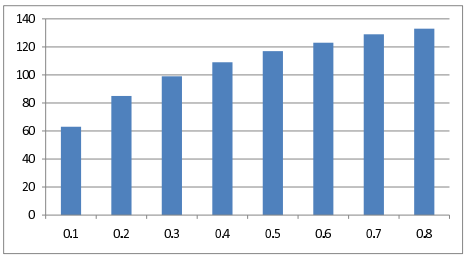

(b) T_0 vs γ

FIGURE 2. Extinction time (T_0) vs mortality rate (δ) and yield constant (γ).

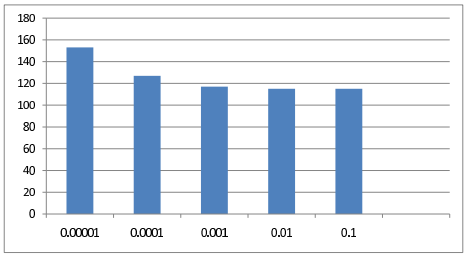

(a) single strain case

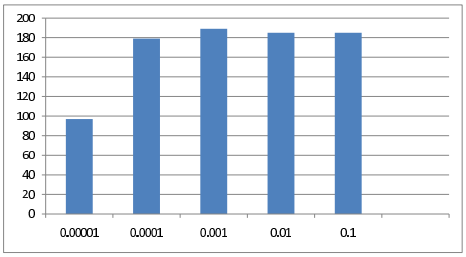

(b) competition case

FIGURE 3. Extinction time (T_0) vs motility (D)-agar case.

3.3. **Computation of extinction time.** Extinction is the end of an organism or group of species. The extinction threshold ϵ_0 is defined as the minimum total density of bacteria, below which bacteria go extinct. We define the extinction time T_0 as the maximum time for the total density of bacteria to stay above the extinction threshold. We analyze the dependence of the extinction time T_0 on δ (death rate) (see Fig.2(a)) and γ (yield constant) (see Fig.2(b)) and D (motility rate) (see Figs.3-4). The total density of bacteria over the space is defined as $\widetilde{B(.)} = \int_\Omega B(\overline{x}, .)d\overline{x}$.

Fig.2 directly follows common sense: when the mortality rate increases, the extinction time decreases (see panel (a)); when the yield constant increases, the extinction time increases (see panel (b)). According to Fig.3, for the agar media, larger motility results in shorter survival of a single strain, while larger motility of motile strain prolongates the extinction time of the motile strain in competition with the immotile strain. More nutrients consuming by bacterial species leads to higher population death. Intrinsic fluctuations and traveling wave speeds also lead to extinction. For a single species (no competition), increasing motility is not favorable, because single strain goes extinct faster if it consumes more nutrients by spreading out. However, in the case of two competing species, the motile strain gets more nutrient, leading to the earlier extinction of the immotile strain. Competition case should be better than single species case. According to Fig.4, for the liquid case, the extinction time is almost independent of motility because liquid nutrients move almost infinitely fast. Two species competition models will be clearly presented in section 4.

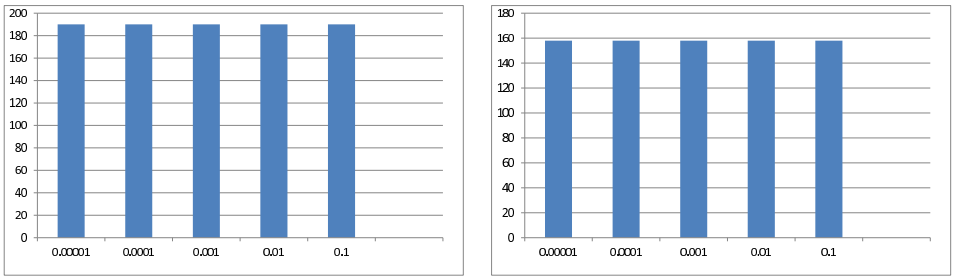

(a) single strain case (b) competition case

FIGURE 4. Extinction time (T_0) vs motility rate (D)-liquid case.

4. **Two competing bacterial species in a petri dish.** We start with two species competing for the same nutrients in one-dimensional space. These species are genetically identical except for their movement speed: the first strain is motile while the second one is immotile. Culture medium ranges from agar to liquid. We perform mathematical analysis including global stability for non-special case and the existence of traveling-wave solutions.

We consider the following reaction-diffusion competition spatial model for agar media:

$$\begin{aligned} \frac{\partial B_1}{\partial t} &= D_1 \Delta B_1 + [h_1(N) - \delta_1] B_1, \\ \frac{\partial B_2}{\partial t} &= D_2 \Delta B_2 + [h_2(N) - \delta_2] B_2, \\ \frac{\partial N}{\partial t} &= -\frac{1}{\gamma_1} h_1(N) B_1 - \frac{1}{\gamma_2} h_2(N) B_2, \end{aligned} \tag{2}$$

where $h_i(N) = \frac{\alpha_i N}{k_i + N}$.
$B_1(x,t)$-density of motile strain; $B_2(x,t)$-density of immotile strain;
D_1-diffusion constant of motile strain; D_2-diffusion constant of immotile strain; $D_1 >> D_2$;
$\alpha_1 = \alpha_2$ - maximum resource uptake rates;
$k_1 = k_2$ - half-saturation constants for resource uptake (representing resource uptake efficiencies);
$\delta_1 = \delta_2$ - bacterial mortality rates;
$\gamma_1 = \gamma_2$ - yield coefficient (mass of viable cells produced per unit of nutrient).

4.1. **Mathematical analysis.** We first consider the following ODE model

$$\begin{aligned} \frac{dB_1}{dt} &= [h_1(N) - \delta_1] B_1, \\ \frac{dB_2}{dt} &= [h_2(N) - \delta_2] B_2, \\ \frac{dN}{dt} &= -\frac{1}{\gamma_1} h_1(N) B_1 - \frac{1}{\gamma_2} h_2(N) B_2. \end{aligned} \tag{3}$$

For this ODE model, we have the following global stability result, which states that eventually the nutrient density approaches some equilibrium level.

Theorem 4.1. *The equilibrium line* $(0, 0, \zeta)$*, where* ζ *is an arbitrary nonnegative number, is globally attracting.*

For the spatial model, the following theorem summarizes the necessary condition for the existence of traveling-wave solutions for system (2).

Theorem 4.2. *The necessary condition for existence of traveling-wave solutions for the agar model (2) is*

$$\sqrt{\frac{D_1^2(\delta_2 - h_2) + D_2^2(\delta_1 - h_1)}{(D_1 + D_2)}} \geq c \geq \frac{\mid D_1(h_2 - \delta_2) - D_2(h_1 - \delta_1) \mid}{\sqrt{(D_1 + D_2)(\delta_1 + \delta_2 - h_1 - h_2)}}.$$

Investigating traveling wave solutions in competition allows us to understand how the nutrients can be ruled by the bacterial strains. Our system admits traveling wave solutions depending on the initial condition. When the nutrients stay at their stable state in the petri dish, adding bacterial strains may result in a "wave of transition" of bacterial strains. We obtain maximum and minimum traveling speeds for traveling-wave solutions.

4.2. **Numerical simulations.** One goal of numerical simulations is to determine whether our theoretical results are consistent to experimental results in [28]. We run simulations in one-dimensional and two-dimensional spaces to illustrate the data fitting. Simulation results in one-dimensional space were obtained using MATLAB, and simulation results in two-dimensional space were obtained using COMSOL. For all the simulations, zero flux boundary conditions were used. Furthermore, we compute extinction times of bacteria, traveling-wave solutions, and ratios of total densities of the two competing strains. We estimate the reasonable ranges of parameters from literature (see Table 1). We choose proper parameter values from these ranges to run simulations.

We start with the simulations on one-dimensional space. We place motile and immotile bacterial strains in the middle of the petri dish and observe competition outcomes (see Fig.5). We select parameter values from the corresponding ranges given in Table 1 [1, 3, 14, 19, 26, 13, 11]: $\alpha_1 = \alpha_2 = 0.6$, $k_1 = k_2 = 0.06$, $\delta_1 = \delta_2 = 0.03$, $\gamma_1 = \gamma_2 = 0.5$, $D_1 = 0.002$, $D_2 = 0.0002$, and the initial conditions: $B_1(x,0) = \begin{cases} 0.05, & |x - 0.5| \leq 0.03; \\ 0, & |x - 0.5| > 0.03; \end{cases}$ $B_2(x,0) = \begin{cases} 0.05, & |x - 0.5| \leq 0.03; \\ 0, & |x - 0.5| > 0.03; \end{cases}$ and $N(x,0) = 0.5$ (high resource) or 0.05 (low resource).

From Fig.5, initially, both strains grow in the middle. After a few hours the motile strain moves out and grows on the boundary, while the immotile strain grows quickly in the middle. And finally both strains die out due to the nutrient-closed system. Fig.6 illustrates that the motile strain is dominant in total density (integration of density over space). After half a day, the ratio of motile strain to immotile strain is around $10 : 1$ (see Fig.9). This result is consistent to the experimental data of the agar case [28]. Fig.5 shows the spatial distributions of both bacterial strains and resource over time.

Now we run a simulation on two-dimensional space. We place one drop of motile strain in the middle of the petri dish and one drop of immotile strain a bit away from the middle. We compute the density distributions of both strains and resource over time, and record these spatial distributions at 0hr, 12hrs, 15hrs and 20hrs in Fig.11. Following Table 1, we choose: $\alpha_1 = \alpha_2 = 0.6$, $k_1 = k_2 = 0.04$, $\delta_1 = \delta_2 = 0.03$, $\gamma_1 = \gamma_2 = 0.5$, $D_1 = 0.002$, $D_2 = 0.0002$. Note that the unit of diffusion coefficients

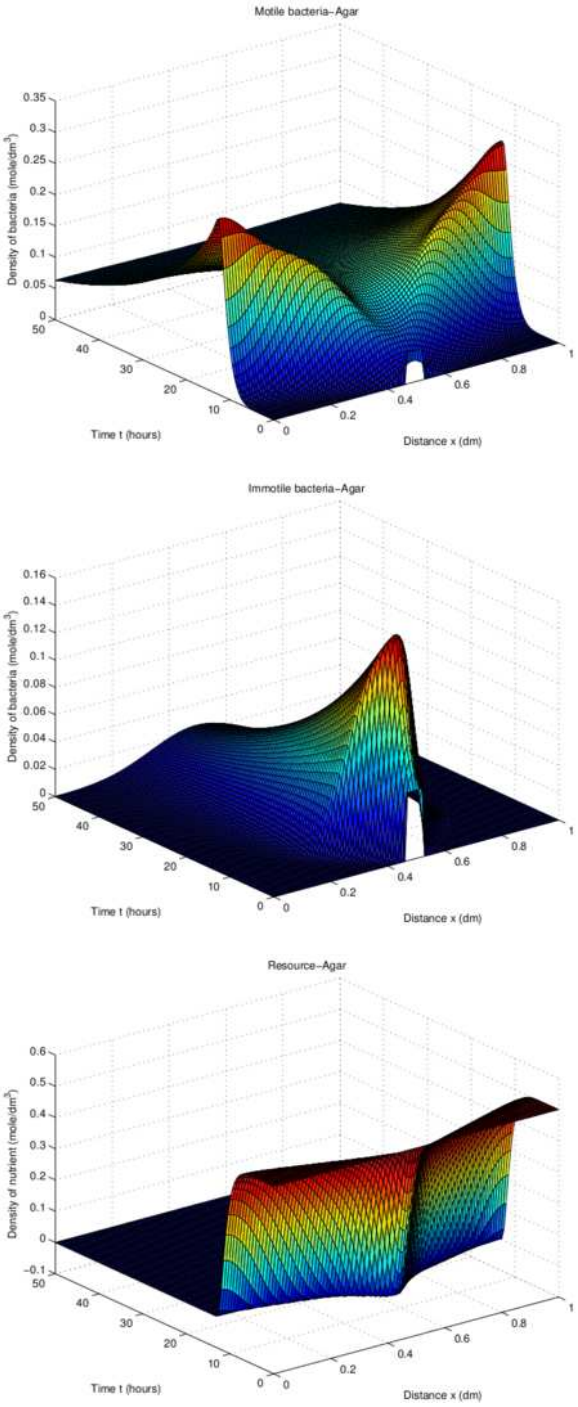

FIGURE 5. One dimensional simulation for the competition of motile and immotile strains in a homogeneous nutrient environment - agar case. Chosen values of parameters are $\alpha_1 = \alpha_2 = 0.6h^{-1}$, $k_1 = k_2 = 0.04(dm)^{-3}$, $\delta_1 = \delta_2 = 0.03h^{-1}$, $\gamma_1 = \gamma_2 = 0.5$, $D_1 = 0.002(dm)^2h^{-1}$, $D_2 = 0.0002(dm)^2h^{-1}$, $N(x,0) = 0.5$.

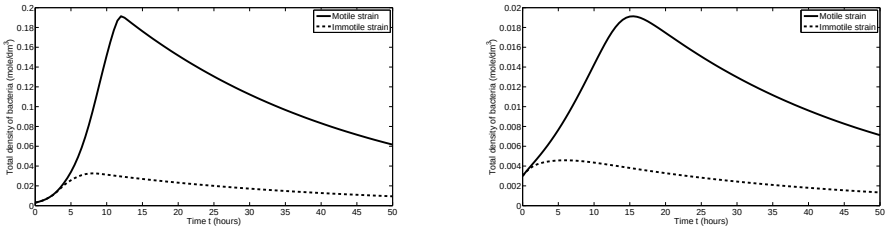

(a) high resource-agar (b) low resource-agar

FIGURE 6. Total densities of motile and immotile strains in one dimensional agar case. Solid and dash lines represent total density of motile and immotile strains. (a) high resource. (b) low resource. Chosen values of parameters are $\alpha_1 = \alpha_2 = 0.6h^{-1}$, $k_1 = k_2 = 0.04(dm)^{-3}$, $\delta_1 = \delta_2 = 0.03h^{-1}$, $\gamma_1 = \gamma_2 = 0.5$, $D_1 = 0.002(dm)^2h^{-1}$, $D_2 = 0.0002(dm)^2h^{-1}$, $N(x,0) = 0.5$.

in two-dimensional space is different from that in one-dimensional space. We choose the following initial conditions to run a simulation in COMSOL:

$$\begin{aligned} B_1(x,y,0) &= \exp[(-(x-0.5)^2-(y-0.5)^2)/0.0001], \\ B_2(x,y,0) &= \exp[(-(x-0.4)^2-(y-0.5)^2)/0.0001], \\ N(x,y,0) &= 0.5. \end{aligned}$$

We use these initial conditions to mimic two drops of bacteria in the petri dish. Actually after a very short time, two drops will become these initial functions for bacterial densities. Note that these initial conditions are similar to those in one-dimensional space.

To mimic experiments, we start our simulation (Fig.11) at time $t = 0$. Motile and immotile strains start to grow on the same position as placed, and the density of the immotile strain is higher than the density of the motile strain. After twelve hours, the density of the immotile strain starts to decrease and the density of motile strain starts to increase. After fifteen hours, the motile strain moves out and grows mainly outside the middle region, and a heterogeneous pattern occurs. After twenty hours, the motile strain grows everywhere and dominates most of the petri dish, the immotile strain has very low density (even in the middle region) due to lack of resource, and most nutrients are used but actually some remain according to Theorem 3.3. However, in real experiments the density of nutrients can be extremely low.

4.3. **Competition in liquid media.** We consider two bacterial strains, genetically identical except for their motility, in a finite one-dimensional space, with homogeneous diffusible liquid nutrient. The model is provided by

$$\begin{aligned} \frac{\partial B_1}{\partial t} &= D_1 \Delta B_1 + [h_1(N) - \delta_1]\, B_1, \\ \frac{\partial B_2}{\partial t} &= D_2 \Delta B_2 + [h_2(N) - \delta_2]\, B_2, \\ \frac{\partial N}{\partial t} &= D_3 \Delta N - \frac{1}{\gamma_1} h_1(N) B_1 - \frac{1}{\gamma_2} h_2(N) B_2, \end{aligned} \tag{4}$$

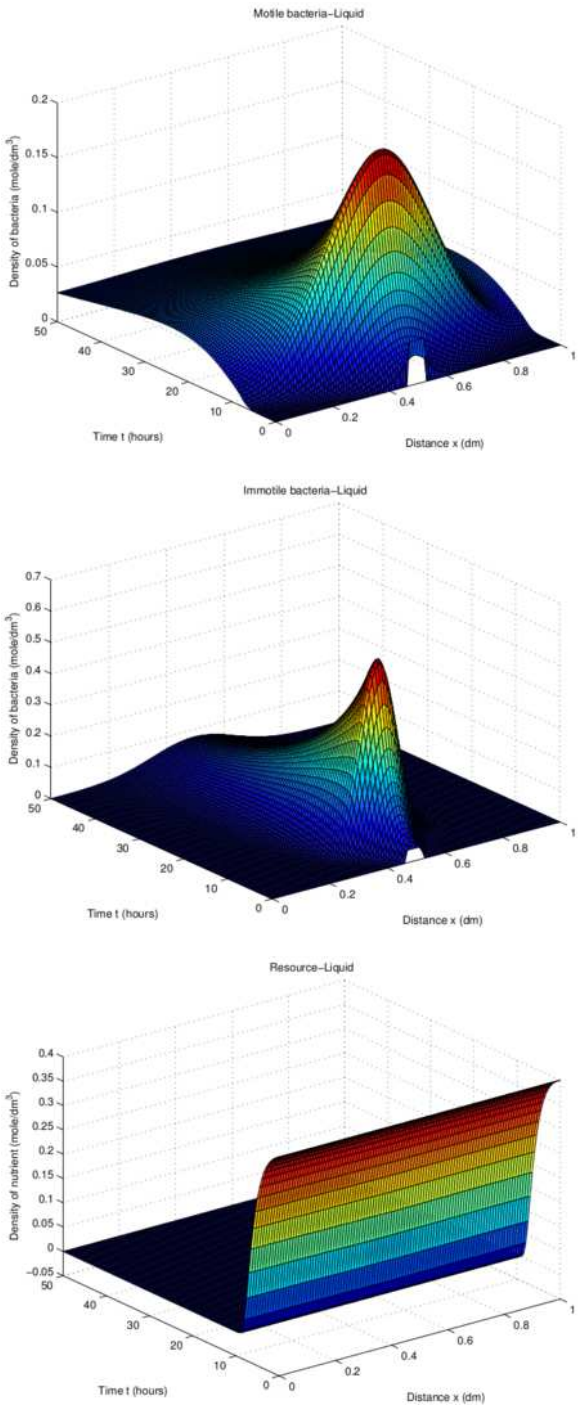

FIGURE 7. One dimensional simulation for the competition of motile and immotile strains in a homogeneous nutrient environment - liquid case. Chosen values of parameter are $\alpha_1 = \alpha_2 = 0.6h^{-1}$, $k_1 = k_2 = 0.04(dm)^{-3}$, $\delta_1 = \delta_2 = 0.03h^{-1}$, $\gamma_1 = \gamma_2 = 0.5$, $D_1 = 0.002(dm)^2h^{-1}$, $D_2 = 0.0002(dm)^2h^{-1}$, $D_3 = 4(dm)^2h^{-1}$.

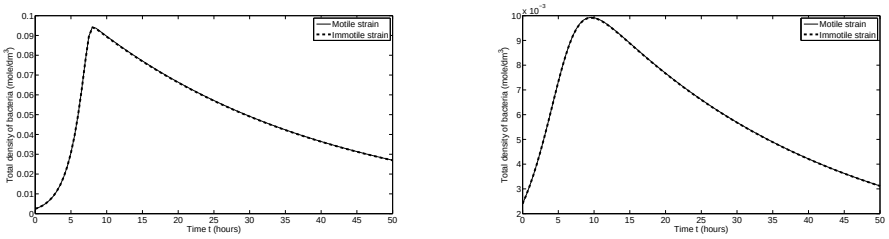

(a) high resource-liquid (b) low resource-liquid

FIGURE 8. Total densities of motile and immotile strains in one dimensional liquid case. Solid and dash lines represent total density of motile and immotile strains. (a) high resource. (b) low resource. Chosen values of parameters are $\alpha_1 = \alpha_2 = 0.6h^{-1}$, $k_1 = k_2 = 0.04(dm)^{-3}$, $\delta_1 = \delta_2 = 0.03h^{-1}$, $\gamma_1 = \gamma_2 = 0.5$, $D_1 = 0.002(dm)^2h^{-1}$, $D_2 = 0.0002(dm)^2h^{-1}$, $D_3 = 4(dm)^2h^{-1}$.

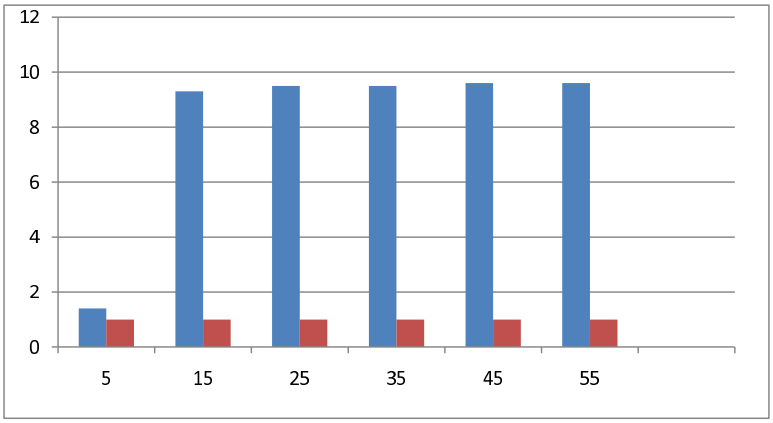

FIGURE 9. Quantitatively fitting the ratio data by computing the total density ratio of motile strain to immotile strain (M/IM) from simulations. The x-axis is time (hrs), and the y-axis is extinction time ($T0$). The first column (blue) at each time plots the ratio for the agar case, and the second column (red) at each time plots the ratio for the liquid case.

where the nutrient diffusion coefficient $D_3 >> D_1 >> D_2$. Pattern formation in liquid is not as interesting as in agar. Numerical simulations in this section show liquid media competition results including spatial distribution over time, total densities, and extinction times.

We consider the simulations on one-dimensional space. Similar to the agar case, we place motile and immotile bacterial strains in the middle of the petri dish and observe competition outcomes in Fig.7. Following Table 1, we choose:

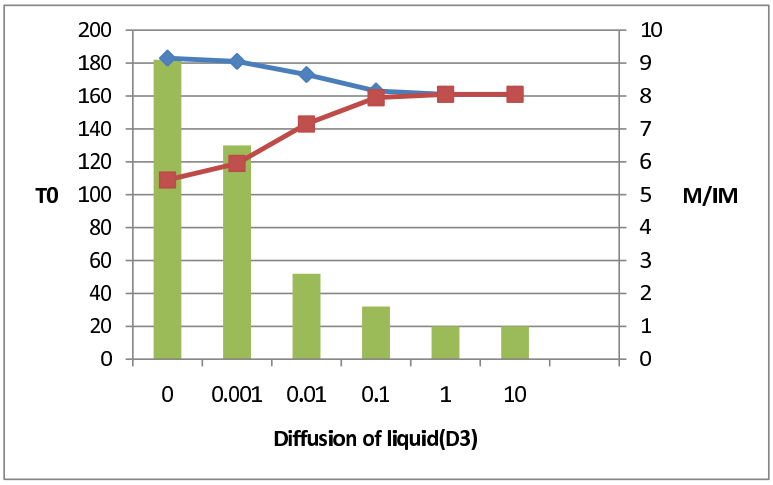

FIGURE 10. The dependence of the density ratio M/IM and the extinction times on the nutrient diffusion rate D_3. The two curves plot extinction times of motile strain (diamond) and immotile strain (square). The bars plot the ratios of motile/immotile strains at $t = 15$ under different nutrient diffusion rates.

$\alpha_1 = \alpha_2 = 0.6$, $k_1 = k_2 = 0.06$, $\delta_1 = \delta_2 = 0.03$, $\gamma_1 = \gamma_2 = 0.5$, $D_1 = 0.002$, $D_2 = 0.0002$, $D_3 = 4$, and initial conditions: $B_1(x,0) = \begin{cases} 0.04, & |x-0.5| \le 0.03; \\ 0, & |x-0.5| > 0.03; \end{cases}$ $B_2(x,0) = \begin{cases} 0.04, & |x-0.5| \le 0.03; \\ 0, & |x-0.5| > 0.03; \end{cases}$ and $N(x,0) = 0.4$ (high resource) or 0.04 (low resource).

The motile strain moves out only a bit more than the immotile strain. Actually, both strains grow around the middle of the petri dish (see Fig.7) and have almost the same density (see Fig.8). In the liquid case, bacterial motility is useless because liquid nutrients move almost infinitely fast compared to bacterial movement. When the nutrient density becomes low in the middle, liquid nutrient spreads inward to the middle. Thus, the motile strain has no advantage in liquid media (see Fig.8). The ratio of motile strain to immotile strain is around $1:1$ (see Fig.9). It is almost consistent to the experimental data of the liquid case [28].

In Fig.10, we vary the nutrient diffusion coefficient D_3 from 0 to 10 in log scale, in which interval agar and liquid media are two extremes, to examine how the resource type determines the ratio of the motile strain to the immotile strain and extinction times of both strains. The ratio of the motile strain to the immotile strain at $t = 15$ decreases as D_3 increases. The extinction time of the motile strain decreases and that of the immotile strain increases as D_3 increases, and the extinction times of both strains coincide when D_3 is large enough ($D_3 > 1$).

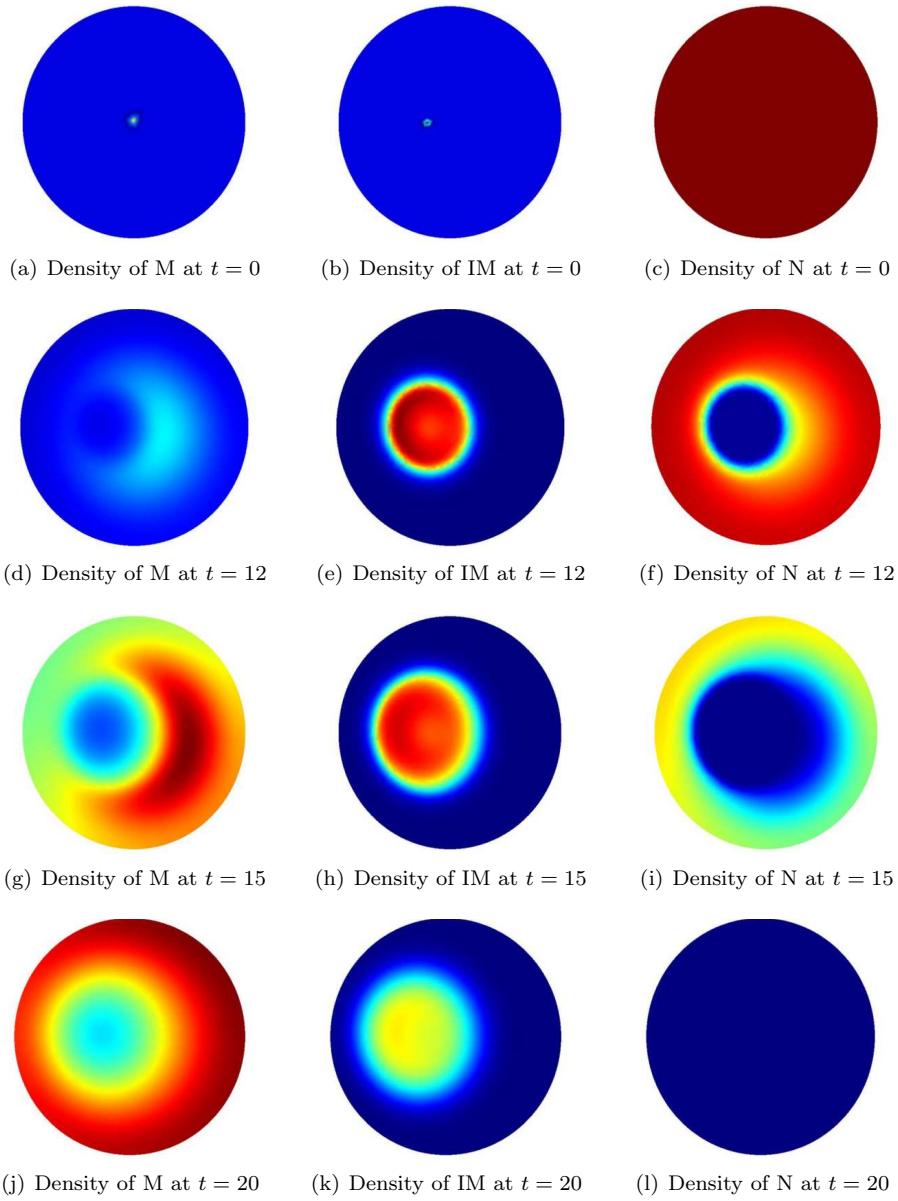

(a) Density of M at $t = 0$ (b) Density of IM at $t = 0$ (c) Density of N at $t = 0$

(d) Density of M at $t = 12$ (e) Density of IM at $t = 12$ (f) Density of N at $t = 12$

(g) Density of M at $t = 15$ (h) Density of IM at $t = 15$ (i) Density of N at $t = 15$

(j) Density of M at $t = 20$ (k) Density of IM at $t = 20$ (l) Density of N at $t = 20$

FIGURE 11. Two dimensional simulations ($2 - D$ figures) at $t = 0, 12, 15, 20$. M represents the motile strain, IM represents the immotile strain and N represents the nutrients. In these figures, the dark red color represents high bacterial densities, the blue color represents almost zero densities, and the color changing from dark red to blue represents the density of bacterial strain changing from high to low.

TABLE 1. Variables and Parameters

Var/Par	Definition	Unit	Value	Reference
B_1	Density of motile bacteria	$\mathrm{M}(dm)^{-3}$	-	-
B_2	Density of immotile bacteria	$\mathrm{M}(dm)^{-3}$	-	-
N	Density of nutrient	$\mathrm{M}(dm)^{-3}$	-	-
D_1	Diffusion coefficient of motile bacteria	$(dm)^2h^{-1}$	$D_2 - 0.36$	[14, 11]
D_2	Diffusion coefficient of immotile bacteria	$(dm)^2h^{-1}$	$0 - 0.036$	[14, 11]
α_i	Resource uptake rates	h^{-1}	$0.02 - 0.86$	[14, 3, 26, 13]
δ_i	Bacterial mortality rates	h^{-1}	$0.01 - 0.07$	[14, 3]
γ_i	Yield constants	-	0.5	[14, 11]
k_i	Half-saturation constants	$\mathrm{mole}(dm)^{-3}$	$0.001 - 0.08$	[14, 19, 1]
D_3	Diffusion coefficient of nutrient	$(dm)^2h^{-1}$	$>> D_1 > 0$	[12]

5. **Discussion.** In this paper, we study a mathematical model for competition of motile and immotile bacterial strains in a homogeneous nutrient environment, with the purpose of exploring the role of nutrient and random (undirected) motility in bacterial competition. Directed motility of bacteria (chemotaxis) has been widely studied empirically and theoretically. The undirected motility was thought to be unimportant and thus was rarely examined specifically in literature about bacterial competition. However, undirected motility can be more important in resource-homogeneous environments. Motivated by a series of lab experiments [28], we discuss the theoretical aspects of the undirected motion of bacteria in this paper.

Our theoretical framework shows even though nutrients always exist, eventually bacteria will go extinct when lack of nutrients. If we incorporate a nutrient input as chemostat-type models (nutrient-open), then the bacterial community can be sustained. We show the existence of traveling-wave solutions by additionally providing their minimum and maximum traveling speeds. The minimum or maximum spreading rate is an increasing function with respect to diffusion coefficient. Thus, the existence of traveling wave solutions provide a lower and an upper bound for the bacterial spreading rate. This result seems novel because almost all previous models show that traveling-wave solutions have a minimum traveling speed.

Using numerical simulations, we show that in agar media the motile strain grows on the boundary after a few hours, but in liquid media it always grows in the middle. In both media the immotile strain grows in the middle, and it has much higher total density in liquid media than in agar media. In agar media the motile strain is dominant in total density, while in liquid media bacterial motility is not that important. This result is consistent with experimental data [28]. Simulation and experimental results illustrate the advantage of undirected motility in agar media and in the absence of chemotaxis.

Our theoretical framework is based on coupled reaction-diffusion-type equations with multiple assumptions, such as undirected motility without chemotaxis, genetically identical bacterial strains except motility, and one type of resource. We construct and discuss a PDE model in the explicit consideration of nutrient and different bacterial strains characterized by motility. In liquid media, if we assume that immotile strain utilizes nutrient more efficiently than the motile strain ($k_1 > k_2$) due to energy cost of movement, then the total density ratio of motile strain to immotile strain is far less than one. Models in two-dimensional space are enough to mimic the petri dish experiment [28], although some applications such as biofilm in teeth and bath tub may need three-dimensional space.

More theoretical work and lab experiments need to be accumulated to validate undirected motility in bacteria and its effects on competition. The assumptions of the existing models require further verification in experiments. Some well organized lab experiments in heterogeneous nutrient environments will be important to understand the significance of undirected (random) cell movement.

Appendix.

Proof of Theorem 3.1 We consider the one-dimensional space case and the two-dimensional space (disk petri dish) case separately.

For spatially uniform steady states, where solutions are independent of time and space, we have the following algebraic equations:

$$\begin{aligned} (h(N) - \delta)B &= 0, \\ -\frac{1}{\gamma}h(N)B &= 0, \end{aligned} \tag{5}$$

the second equation of (5) implies $B = 0$ or $N = 0$.

If $B = 0$, then $N \geq 0$.

If $N = 0$, substituting it into the first equation of (5) leads to $B = 0$.

For spatially non-uniform steady states, where solutions are independent of time, we have the following equations:

$$\begin{aligned} D\frac{d^2B}{dx^2} + (h(N) - \delta)B &= 0, \\ -\frac{1}{\gamma}h(N)B &= 0, \end{aligned} \tag{6}$$

the second equation of (6) implies $B = 0$ or $N = 0$.

If $B = 0$, then $N \geq 0$.

If $N = 0$, then substituting it into the first equation of (6) leads to

$$D\frac{d^2B}{dx^2} - \delta B = 0. \tag{7}$$

From steady states we can see that $B(x) = 0$ is always a solution of the above equation. Therefore we shall look for solutions other than the trivial zero solution. Let $B = e^{wx}$, where w is a constant ready to be determined, then equation (7) leads to $w^2 - \frac{\delta}{D} = 0$, and thus the solution is

$$B = C_1 e^{wx} + C_2 e^{-wx}. \tag{8}$$

One important characteristic of a boundary value problem is that it may not have a solution, while the initial value problem always has a solution and the solution is unique. The equation (7) has no solution when $\delta/D < 0$. If the equation (7) has a

solution, then

$$B = C_1 e^{\sqrt{\frac{\delta}{D}}x} + C_2 e^{-\sqrt{\frac{\delta}{D}}x} \tag{9}$$

for some constants C_1 and C_2 and we can solve the constants using boundary conditions $\frac{\partial B}{\partial x}(0,t) = \frac{\partial B}{\partial x}(L,t) = 0$. Thus $C_1 = C_2 = 0$. Therefore equation (7) has only zero solution.

Now we consider the single species model in a petri dish Ω (disk shape):

$$\begin{aligned} \frac{\partial B}{\partial t} &= D(B_{xx} + B_{yy}) + (h(N) - \delta)B, \\ \frac{\partial N}{\partial t} &= -\frac{1}{\gamma}h(N)B, \end{aligned} \tag{10}$$

or equivalently in polar coordinates

$$\begin{aligned} \frac{\partial B}{\partial r} &= D(B_{rr} + \frac{1}{r}B_r + \frac{1}{r^2}B_{\theta\theta}) + (h(N) - \delta)B, \\ \frac{\partial N}{\partial r} &= -\frac{1}{\gamma}h(N)B. \end{aligned} \tag{11}$$

Spatially uniform steady states are similar to the one-dimensional space case. Now we discuss spatially non-uniform steady states.
The second equation of (11)implies $B = 0$ or $N = 0$.
If $B = 0$ then $N \geq 0$.
If $N = 0$, substituting it into the first equation of (11) leads to

$$B_{rr} + \frac{1}{r}B_r + \frac{1}{r^2}B_{\theta\theta} - \frac{\delta}{D}B = 0, \tag{12}$$

with r dependent boundary conditions

$$\frac{\partial B}{\partial r}(a,\theta) = 0, \qquad |B(0,\theta)| < \infty,$$

and θ dependent boundary conditions

$$B(r,\pi) = B(r,-\pi), \qquad \frac{\partial B}{\partial \theta}(r,\pi) = \frac{\partial B}{\partial \theta}(r,-\pi).$$

Consider the product solution

$$B(r,\theta) \quad = \quad R(r)\Theta(\theta),$$

where θ is a polar angle with

$$\Theta(\theta + 2\pi) = \Theta(\theta).$$

Plugging the product solution into the equation, we find

$$\begin{aligned} R''\Theta + \frac{1}{r}R'\Theta + \frac{1}{r^2}R\Theta'' - \frac{\delta}{D}R\Theta = 0 \\ \Rightarrow \Theta(R'' + \frac{1}{r}R' - \frac{\delta}{D}R) = -\frac{1}{r^2}R\Theta'' \\ \Rightarrow r^2\frac{R''}{R} + r\frac{R'}{R} - r^2\frac{\delta}{D}R = -\frac{\Theta''}{\Theta} = \lambda \qquad \text{where } \lambda \text{ is a separation constant.} \end{aligned}$$

Hence

$$\begin{aligned} r^2\frac{R''}{R} + r\frac{R'}{R} - r^2\frac{\delta}{D}R = \lambda \qquad \text{and} \\ -\frac{\Theta''}{\Theta} = \lambda. \end{aligned} \tag{13}$$

The second equation of (13) implies

$$\Theta'' + \lambda\Theta = 0.$$

The Θ equation has 2π-periodic solutions if and only if

$$\lambda = n^2, \qquad n = 0, \pm 1, \pm 2, ...$$

This leads to the equation

$$\Theta'' + n^2\Theta = 0 \qquad \text{and} \qquad r^2\frac{R''}{R} + r\frac{R'}{R} - r^2\frac{\delta}{D}R = n^2$$

with

$$\Theta(\pi) = \Theta(-\pi), \qquad \frac{\partial\Theta}{\partial\theta}(\pi) = \frac{\partial\Theta}{\partial\theta}(-\pi).$$

We know that the eigenvalues are $\lambda = n^2$ for $n = 0, 1, \cdots$, although it is not a regular Sturm-Liouville problem due to the periodic boundary conditions. The corresponding eigenfunctions are $\Theta(\theta) = \sin n\theta$ and $\Theta(\theta) = \cos n\theta$. Hence, the general ODE has the form

$$\Theta(\theta) \quad = \quad c_5 \cos n\theta + c_6 \sin(n\theta), \qquad n \text{ integer.}$$

On the other hand,

$$r^2R'' + rR' + \left(-\frac{\delta}{D}r^2 - n^2\right)R \quad = \quad 0 \qquad \text{with} \tag{14}$$

$$\frac{\partial R}{\partial r}(a) = 0, \qquad |R(0)| < \infty.$$

Equation (14) looks similar to Bessel's differential equation, but it has the opposite sign in front of the r^2 term. If we let

$$q = \left(\frac{\delta}{D}\right) r,$$

then the equation (14) becomes

$$q^2\frac{\partial^2 R}{\partial q^2} + q\frac{\partial R}{\partial q} + (-q^2 - n^2)R \quad = \quad 0,$$

which is a modified Bessel's differential equation, and the solution is

$$R \quad = \quad c_3 K_n\left(\frac{\delta}{D}r\right) + c_4 I_n\left(\frac{\delta}{D}r\right),$$

where

$$K_n = \frac{\pi}{2}\frac{I_{-n}(q) - I_n(q)}{\sin(n\pi)} \qquad \text{and} \qquad I_n = \sum_{p=1}^{\infty}\frac{(q/2)^{n+2p}}{p!(p+n)!}.$$

Using the boundary condition $|R(0)| < \infty$ and since K_n is singular at $r = 0$ and I_n is not, it follows that $c_3 = 0$ and $R(r)$ is proportional to $I_n\left(\frac{\delta r}{D}\right)$. Note that both $K_n(q)$ and $I_n(q)$ are non-oscillatory and are nonzero for $q > 0$.
Therefore,

$$R(r, \theta) \quad = \quad c_4 I_n\left(\frac{\delta r}{D}\right).$$

The boundary condition $\frac{\partial R}{\partial r}(a, \theta) = 0$ implies that

$$\frac{\delta}{D}c_4 I_n'\left(\frac{\delta}{D}a\right) \quad = \quad 0,$$

which leads to

$$c_4 \frac{I_{n-1}\left(\frac{\delta}{D}a\right) + I_{n+1}\left(\frac{\delta}{D}a\right)}{2} = 0.$$

Since $I_{n-1}\left(\frac{\delta}{D}a\right)$ and $I_{n+1}(\frac{\delta}{D}a)$ are nonzero for $a > 0$, we have $c_4 = 0$. Consequently, the equation (12) has only zero solution ($\delta > 0$, $D > 0$).

From spatially uniform steady states and spatially non-uniform steady states, we conclude that for both one-dimensional and two-dimensional cases, if $B = 0$ then $N \geq 0$ and if $N = 0$ then $B = 0$. □

Proof of Theorem 3.2 We look for traveling-wave solutions of the form

$$B(t,x) = \bar{B}(\eta), \qquad N(t,x) = \bar{N}(\eta),$$

where $\eta = x - ct$. With this specific form of traveling waves, the PDE system becomes an ODE system:

$$\begin{aligned} -c\frac{d\bar{B}}{d\eta} &= D\frac{d^2\bar{B}}{d\eta^2} + (h(\bar{N}) - \delta)\bar{B}, \\ -c\frac{d\bar{N}}{d\eta} &= -\frac{1}{\gamma}h(\bar{N})\bar{B}, \end{aligned} \tag{15}$$

Letting $\frac{d\bar{B}}{d\eta} = R$, the equation (15) can be written as a system of first-order ODEs:

$$\begin{aligned} \frac{d\bar{B}}{d\eta} &= R, \\ \frac{dR}{d\eta} &= -\frac{c}{D}R - \frac{h(\bar{N}) - \delta}{D}\bar{B}, \\ \frac{d\bar{N}}{d\eta} &= \frac{1}{\gamma c}\bar{B}h(\bar{N}), \end{aligned} \tag{16}$$

and the critical points are all points on the $\bar{N}$ axis.

Integrating equation (15) from $-\infty$ to $+\infty$, we have

$$-c[\bar{B}]_{-\infty}^{+\infty} = D\left[\frac{dB}{d\eta}\right]_{-\infty}^{+\infty} + \int_{-\infty}^{+\infty}(h(\bar{N}) - \delta)\bar{B}d\eta,$$

$$\int_{-\infty}^{+\infty}(h(\bar{N}) - \delta)\bar{B}d\eta = 0 \qquad (\text{ since } B \to 0 \text{ as } x \to \pm\infty), \tag{17}$$

$$-c[\bar{N}]_{-\infty}^{+\infty} = -\frac{1}{\gamma}\int_{-\infty}^{+\infty} h(\bar{N})\bar{B}d\eta,$$

$$-c(1-n) = -\frac{1}{\gamma}\int_{-\infty}^{+\infty} h(\bar{N})\bar{B}d\eta \tag{18}$$

(since $N \to 1$ as $x \to +\infty$, $N \to n$ as $x \to -\infty$).

Now $\frac{(17)}{\gamma}$+ (18) implies

$$c(1-n) = \frac{1}{\gamma}\int_{-\infty}^{+\infty}\delta\bar{B}d\eta = c\delta\int_n^1 \frac{d\bar{n}}{h(\bar{n})} \qquad (\text{replace } \bar{N} \text{ with } \bar{n} \text{ for integral}).$$

From equation (16), we have

$$\frac{dR}{d\eta} = -\frac{c}{D}\frac{d\bar{B}}{d\eta} - \frac{\gamma c}{D}\frac{d\bar{N}}{d\eta} + \frac{\delta\gamma c}{D}\frac{1}{h(\bar{N})}\frac{d\bar{N}}{d\eta}. \tag{19}$$

Integrating equation (19) from η to $+\infty$ to get

$$\frac{D}{c}R = \phi(\bar{N}) - \bar{B}, \tag{20}$$

where

$$\phi(\bar{N}) = \gamma\left(1 - \bar{N} - \delta\int_{\bar{N}}^{1}\frac{d\bar{n}}{h(\bar{n})}\right). \tag{21}$$

Obviously, we have $\phi(1) = 0$, and from equation (21) we have

$$\phi(\bar{n}) = \gamma\left(1 - \bar{n} - \delta\int_{\bar{n}}^{1}\frac{d\bar{n}}{h(\bar{n})}\right) = \gamma(1 - n - (1 - n)) = 0.$$

This defines a invariant manifold for the system. If a trajectory starts on it, it stays on it, and since

$$\phi(n) = \phi(1) = 0,$$

$(0, 0, n)$, $(0, 0, 1)$ are both on it, we can reduce (16) to the planar system

$$\begin{aligned}\frac{d\bar{B}}{d\eta} &= \frac{c}{D}(\phi(\bar{N}) - \bar{B}),\\ \frac{d\bar{N}}{d\eta} &= (\gamma c)^{-1}\bar{B}h(\bar{N}).\end{aligned} \tag{22}$$

We need to look for eigenvalues at the critical points $(\bar{B}_s, \bar{N}_s)$. The Jacobian matrix of the system (16) is

$$\begin{bmatrix}\bar{B}'\\ \bar{N}'\end{bmatrix} = \begin{bmatrix}-\frac{c}{D} & \frac{c}{D}\phi'(\bar{N})\\ \frac{h(\bar{N})}{\gamma c} & 0\end{bmatrix}\begin{bmatrix}\bar{B}\\ \bar{N}\end{bmatrix},$$

which leads to the characteristic equation at $(\bar{B}_s, \bar{N}_s)$:

$$\lambda^2 + \frac{c}{D}\lambda - \frac{c}{\gamma D}\phi'(\bar{N}_s)h(\bar{N}_s) = 0.$$

The set of eigenvalues for the above matrix is given by

$$\begin{aligned}\lambda_1 &= \frac{-c + \sqrt{c^2 - \frac{4D}{\gamma}\sigma(\bar{N}_s)}}{2D},\\ \lambda_2 &= \frac{-c - \sqrt{c^2 - \frac{4D}{\gamma}\sigma(\bar{N}_s)}}{2D},\end{aligned}$$

where $\sigma(\bar{N}_s) = -h(\bar{N}_s)\phi'(\bar{N}_s)$.

The trajectory representing a wave must approach $(0, 0, n)$ as $\eta \to -\infty$, so it is necessary that one of the eigenvalues has positive real part if $\sigma(n) < 0$. If this is the case, λ_1 and λ_2 are real. Similarly, the trajectory must approach $(0, 0, 1)$ as $\eta \to \infty$. We have the restriction on the wave speed that $c \geq 2(\frac{D\sigma(1)}{\gamma})^{1/2} \equiv c^*$. We

see that $c \geq c^*$ is only the necessary condition, $c \geq c_{min} = c^*$. Hence the minimum traveling-wave speed is $c^* \equiv 2(\frac{D\sigma(1)}{\gamma})^{1/2} \leq c$, where $\sigma(\bar{N}_s) = -h(\bar{N}_s)\phi'(\bar{N}_s)$.□

Proof of Theorem 3.3 The claim follows if we can prove that

$$\int_0^\infty B(\vec{x},t)dt < \infty.$$

Let

$$\mathcal{B}(\vec{x},t) = \int_0^t B(\vec{x},s)ds.$$

Since $\partial\mathcal{B}/\partial t = B$, we can rewrite the first equation of (1) as

$$\frac{\partial^2\mathcal{B}}{\partial t^2} = (D\triangle - \delta)\frac{\partial\mathcal{B}}{\partial t} - \gamma\frac{\partial N}{\partial t},$$

which can be rewritten as

$$\frac{\partial}{\partial t}\left(\frac{\partial\mathcal{B}}{\partial t} - (D\triangle - \delta)\mathcal{B}(\vec{x},t) + \gamma N(\vec{x},t)\right) = 0. \tag{23}$$

Integrating equation (23) to obtain

$$\frac{\partial\mathcal{B}(\vec{x},t)}{\partial t} - (D\triangle - \delta)\mathcal{B}(\vec{x},t) + \gamma N(\vec{x},t) = A(\vec{x}),$$

for some smooth function $A(\vec{x})$. By the sophisticated version of the Method of Variation of Parameters, the solution can be written as

$$\begin{aligned}\mathcal{B}(\vec{x},t) &= \int_0^t e^{(D\triangle-\delta)(t-s)}(A(\vec{x}) - \gamma N(\vec{x},s))ds \leq \int_0^t e^{(D\triangle-\delta)(t-s)}A(\vec{x})ds \\ &= \left(\int_0^t e^{(D\triangle-\delta)(t-s)}ds\right)A(\vec{x}) = (-D\triangle+\delta)^{-1}A(\vec{x}) < \infty.\end{aligned}$$

Integrating the second equation of (1) yields

$$\int_0^t \frac{1}{h(N)}\frac{\partial N}{\partial s}\partial s = \int_0^t -\frac{1}{\gamma}B(\vec{x},s)\partial s. \tag{24}$$

Case I: $h(N) = \alpha N$ Equation (24) implies

$$\int_0^t \frac{\partial N}{N} = \int_0^t -\frac{\alpha}{\gamma}B\partial t = -\frac{\alpha}{\gamma}\mathcal{B},$$

which leads to

$$N(\vec{x},t) = N(\vec{x},0)e^{-\frac{\alpha}{\gamma}\mathcal{B}},$$

that causes a contradiction when $N \to 0$.

Case II: $h(N) = \frac{\alpha N}{k+N}$ Equation (24) implies

$$\int_{N(\vec{x},0)}^{N(\vec{x},t)} \frac{k+N}{N}\partial N = -\frac{\alpha}{\gamma}\mathcal{B},$$

which leads to

$$k(\log N(\vec{x},t) - \log N(\vec{x},0)) + N(\vec{x},t) - N(\vec{x},0) = -\frac{\alpha}{\gamma}\mathcal{B} > -\infty.$$

When $N \to 0$, the left hand side goes to $-\infty$ but the right hand side never goes to $-\infty$, it is a contradiction. □

Remark: Even though the function $h(N)$ satisfies the conditions $h(0) = 0$, $h'(t) > 0$, and $h''(t) \leq 0$, we cannot reach theorem 3.3. Counter example: If $h(N) = \sqrt{N}$, then $h'(N) = \frac{1}{2}N^{-\frac{1}{2}} > 0$ and $h''(N) = -\frac{1}{4}N^{-\frac{3}{2}} < 0$. Hence, we have

$$\int_{N(\vec{x},0)}^{N(\vec{x},t)} N^{-\frac{1}{2}} \partial N = -\frac{1}{\gamma}\mathcal{B}, \tag{25}$$

$$2(N(\vec{x},t)^{\frac{1}{2}} - N(\vec{x},0)^{\frac{1}{2}}) = -\frac{1}{\gamma}\mathcal{B}. \tag{26}$$

When $N \to 0$, the left hand side goes to zero and the right hand side also goes to zero. We cannot obtain Theorem 3.3 using the same approach.

Proof of Theorem 4.1 It is obvious that any point on the line $(0, 0, \zeta), \zeta \geq 0$ is an equilibrium. We will show that there exists $T > 0$ such that $\delta_1 > h_1(N)$ and $\delta_2 > h_2(N)$ when $t > T$, by contradiction.
If this claim is not true, we have $\delta_1 < h_1(N)$ for all t or $\delta_2 < h_2(N)$ for all t. Therefore

$$\frac{dB_1}{dt} \quad \geq \epsilon B_1 \quad \text{for all} \quad t \quad \text{or} \quad \tfrac{dB_2}{dt} \quad \geq \epsilon B_2 \quad \text{for all} \quad t. \tag{27}$$

Integrating equation (27) with respect to t implies

$$B_1 \quad \geq ae^{\epsilon t} \quad \text{for all} \quad t \quad \text{or} \quad B_2 \quad \geq be^{\epsilon t} \quad \text{for all} \quad t.$$

When $t \to \infty$, then $B_1 \to \infty$ or $B_2 \to \infty$. On the other hand, if we consider the Lyapunov function

$$\begin{aligned} V(B_1, B_2, N) &= 1/2(B_1^2 + B_2^2 + N^2), \\ \dot{V}(B_1, B_2, N) &= B_1\dot{B}_1 + B_2\dot{B}_2 + N\dot{N} \\ &= B_1^2(h_1(N) - \delta_1) + B_2^2(h_2(N) - \delta_2) - N(\frac{1}{\gamma_1}h_1(N)B_1 + \frac{1}{\gamma_2}h_2(N)B_2) \\ &< 0, \qquad \text{for} \qquad t > T, \end{aligned}$$

then any solution approaches some point on the line $(0, 0, \zeta), \zeta \geq 0$, that is, the equilibrium line $(0, 0, \zeta), \zeta \geq 0$ is globally attracting. A contradiction. □

Proof of Theorem 4.2 Consider the equations

$$\begin{aligned} \frac{\partial B_1}{\partial t} &= D_1 \triangle B_1 + (h_1(N) - \delta_1)B_1, \\ \frac{\partial B_2}{\partial t} &= D_2 \triangle B_2 + (h_2(N) - \delta_2)B_2, \\ \frac{\partial N}{\partial t} &= -\frac{1}{\gamma_1}h_1(N)B_1 - \frac{1}{\gamma_2}h_2(N)B_2, \end{aligned} \tag{28}$$

Let $B_1(t, x) = B_1(x - ct)$, $B_2(t, x) = B_2(x - ct)$, and $N(t, x) = N(x - ct)$, then the equations become

$$\begin{aligned} -cB_1' &= D_1 B_1'' + (h_1(N) - \delta_1)B_1, \\ -cB_2' &= D_2 B_2'' + (h_2(N) - \delta_2)B_2, \\ -cN' &= -\frac{1}{\gamma_1}h_1(N)B_1 - \frac{1}{\gamma_2}h_2(N)B_2. \end{aligned} \tag{29}$$

Now let $B_1' = B_{11}$ and $B_2' = B_{22}$,

$$\begin{aligned} -cB_{11} &= D_1 B_{11}' + (h_1(N) - \delta_1)B_1, \\ -cB_{22} &= D_2 B_{22}' + (h_2(N) - \delta_2)B_2, \\ -cN' &= -\frac{1}{\gamma_1}h_1(N)B_1 - \frac{1}{\gamma_2}h_2(N)B_2, \end{aligned} \tag{30}$$

and then

$$\begin{aligned} B_{11}' &= \frac{-c}{D_1}B_{11} - \frac{1}{D_1}(h_1(N) - \delta_1)B_1, \\ B_1' &= B_{11}, \\ B_{22}' &= \frac{-c}{D_2}B_{22} - \frac{1}{D_2}(h_2(N) - \delta_2)B_2, \\ B_2' &= B_{22}, \\ N' &= \frac{1}{c\gamma_1}h_1(N)B_1 + \frac{1}{c\gamma_2}h_2(N)B_2. \end{aligned}$$

At critical point $(0, 0, \zeta)$, $\zeta \geq 0$, let $h_1(\zeta) = h_1$ and $h_2(\zeta) = h_2$, the Jacobian matrix is

$$\begin{pmatrix} -c/D_1 & -(h_1 - \delta_1)/D_1 & 0 & 0 & 0 \\ 1 & 0 & 0 & 0 & 0 \\ 0 & 0 & -c/D_2 & -(h_2 - \delta_2)/D_2 & 0 \\ 0 & 0 & 1 & 0 & 0 \\ 0 & \frac{h_1}{c\gamma_1} & 0 & \frac{h_2}{c\gamma_2} & 0 \end{pmatrix}$$

and thus the characteristic polynomial is given by

$$\chi(\lambda) = \begin{vmatrix} -c/D_1 - \lambda & -(h_1 - \delta_1)/D_1 & 0 & 0 & 0 \\ 1 & 0 - \lambda & 0 & 0 & 0 \\ 0 & 0 & -c/D_2 - \lambda & -(h_2 - \delta_2)/D_2 & 0 \\ 0 & 0 & 1 & 0 - \lambda & 0 \\ 0 & \frac{h_1}{c\gamma_1} & 0 & \frac{h_2}{c\gamma_2} & 0 - \lambda \end{vmatrix}.$$

The characteristic equation $\chi(\lambda) = 0$ is

$$\begin{aligned} 0 \quad = \quad & \lambda^5 + (c/D_1 + c/D_2)\lambda^4 + (\frac{c^2}{D_1 D_2} + \frac{(h_1 - \delta_1)}{D_1} + \frac{(h_2 - \delta_2)}{D_2})\lambda^3 \\ & + \frac{c}{D_1 D_2}(h_1 + h_2 - \delta_1 - \delta_2)\lambda^2 + \frac{(h_1 - \delta_1)(h_2 - \delta_2)}{D_1 D_2}\lambda. \end{aligned}$$

We apply the Routh-Hurwitz criterion to obtain the following:

$$\begin{bmatrix} 1 & \frac{c^2}{D_1 D_2} + \frac{(h_1 - \delta_1)}{D_1} + \frac{(h_2 - \delta_2)}{D_2} & \frac{(h_1 - \delta_1)(h_2 - \delta_2)}{D_1 D_2} \\ \frac{c}{D_1} + \frac{c}{D_2} & \frac{c}{D_1 D_2(h_1 + h_2 - \delta_1 - \delta_2)} & 0 \end{bmatrix}$$

$$b_1 = \frac{c^2(D_1 + D_2) + D_1^2(h_2 - \delta_2) + D_2^2(h_1 - \delta_1)}{D_1 D_2(D_1 + D_2)} \qquad b_2 = \frac{(h_1 - \delta_1)(h_2 - \delta_2)}{D_1 D_2} \qquad 0$$

$$c_1 = \frac{c}{D_1 D_2}\frac{\left([D_1(h_2 - \delta_2) - D_2(h_1 - \delta_1)]^2 + c^2(D_1 + D_2)(h_1 + h_2 - \delta_1 - \delta_2)\right)}{c^2(D_1 + D_2) - D_1^2(\delta_2 - h_2) - D_2^2(\delta_1 - h_1)} \qquad 0$$

and $d_1 = b_2$.

If $b_2 > 0$ and $c_1 < 0$ then $(0, 0, \zeta)$ is unstable.

If $b_2 < 0$ and $c_1 > 0$ then $(0, 0, \zeta)$ is unstable.
If $b_2 > 0$ and $c_1 > 0$ then $(0, 0, \zeta)$ is locally asymptotically stable, which imply

$$\frac{(h_1 - \delta_1)(h_2 - \delta_2)}{D_1 D_2} > 0 \tag{31}$$

and

$$\frac{c}{D_1 D_2} \frac{[D_1(h_2 - \delta_2) - D_2(h_1 - \delta_1)]^2 + c^2(D_1 + D_2)(h_1 + h_2 - \delta_1 - \delta_2)}{c^2(D_1 + D_2) - D_1^2(\delta_2 - h_2) - D_2^2(\delta_1 - h_1)} > 0. \tag{32}$$

The first condition (31) leads to two cases:
(i) $(h_1 - \delta_1) > 0$ and $(h_2 - \delta_2) > 0$;
(ii) $(h_1 - \delta_1) < 0$ and $(h_2 - \delta_2) < 0$.
For the case (i) $(h_1 - \delta_1) > 0$ and $(h_2 - \delta_2) > 0$, we have $b_1 > 0$. Thus $(0, 0, \zeta)$ is locally asymptotically stable.
On the other hand, if $(h_1 - \delta_1) > 0$ and $(h_2 - \delta_2) > 0$, then there exists $\xi > 0$ (small enough) such that

$$\frac{\partial B_1}{\partial t} = D_1 \Delta B_1 + (h_1(N) - \delta_1) B_1 \geq D_1 \Delta B_1 + \epsilon B_1,$$
$$\text{for} \quad (B_1(0), B_2(0), N(0)) \in \mathbf{B}_\xi((0, 0, \zeta)),$$

$$\frac{\partial B_2}{\partial t} = D_2 \Delta B_2 + (h_2(N) - \delta_2) B_2 \geq D_2 \Delta B_2 + \epsilon B_2,$$
$$\text{for} \quad (B_1(0), B_2(0), N(0)) \in \mathbf{B}_\xi((0, 0, \zeta)).$$

Differentiating $\widetilde{B(t)} = \int_\Omega B(\vec{x}, \vec{t}) d\vec{x}$ yields

$$\frac{\partial \widetilde{B_1}}{\partial t} \geq \int_\Omega D_1 \Delta B_1 d\vec{x} + \epsilon \widetilde{B_1},$$
$$\frac{\partial \widetilde{B_2}}{\partial t} \geq \int_\Omega D_2 \Delta B_2 d\vec{x} + \epsilon \widetilde{B_2}.$$

The integral is zero due to the zero flux hypothesis and Stoke's theorem. We thus obtain

$$\begin{aligned} \frac{\partial \widetilde{B_1}}{\partial t} &\geq \epsilon \widetilde{B_1}, \\ \frac{\partial \widetilde{B_2}}{\partial t} &\geq \epsilon \widetilde{B_2}. \end{aligned} \tag{33}$$

Integrating equation (33) with respect to t yields

$$\widetilde{B_1} \geq a e^{\epsilon \widetilde{B_1}},$$
$$\widetilde{B_2} \geq b e^{\epsilon \widetilde{B_2}}.$$

It contradicts the result that $(0, 0, \zeta)$ is locally asymptotically stable.
For the case (ii) $(h_1 - \delta_1) < 0$ and $(h_2 - \delta_2) < 0$, the second condition (32) for asymptotic stability leads to

$$\begin{aligned} [D_1(h_2 - \delta_2) - D_2(h_1 - \delta_1)]^2 > c^2(D_1 + D_2)(\delta_1 + \delta_2 - h_1 - h_2) \quad \text{and} \\ c^2(D_1 + D_2) > D_1^2(\delta_2 - h_2) + D_2^2(\delta_1 - h_1), \end{aligned} \tag{34}$$

or

$$\begin{aligned}[D_1(h_2-\delta_2)-D_2(h_1-\delta_1)]^2 < c^2(D_1+D_2)(\delta_1+\delta_2-h_1-h_2) \quad \text{and} \\ c^2(D_1+D_2) < D_1^2(\delta_2-h_2)+D_2^2(\delta_1-h_1).\end{aligned} \tag{35}$$

Equations (34) and (35) are equivalent to

$$\frac{D_1^2(\delta_2-h_2)+D_2^2(\delta_1-h_1)}{(D_1+D_2)} < c^2 < \frac{[D_1(h_2-\delta_2)-D_2(h_1-\delta_1)]^2}{(D_1+D_2)(\delta_1+\delta_2-h_1-h_2)} \tag{36}$$

or

$$\frac{D_1^2(\delta_2-h_2)+D_2^2(\delta_1-h_1)}{(D_1+D_2)} > c^2 > \frac{[D_1(h_2-\delta_2)-D_2(h_1-\delta_1)]^2}{(D_1+D_2)(\delta_1+\delta_2-h_1-h_2)}. \tag{37}$$

To show the following inequality

$$\frac{D_1^2(\delta_2-h_2)+D_2^2(\delta_1-h_1)}{(D_1+D_2)} \geq \frac{[D_1(h_2-\delta_2)-D_2(h_1-\delta_1)]^2}{(D_1+D_2)(\delta_1+\delta_2-h_1-h_2)},$$

we only need to show that

$$[D_1^2(\delta_2-h_2)+D_2^2(\delta_1-h_1)](\delta_1+\delta_2-h_1-h_2) \geq [D_1(h_2-\delta_2)-D_2(h_1-\delta_1)]^2.$$

Now

$$LHS = D_1^2(\delta_2-h_2)(\delta_1-h_1)+D_1^2(\delta_2-h_2)^2+D_2^2(\delta_1-h_1)(\delta_2-h_2)+D_2^2(\delta_1-h_1)^2,$$

$$RHS = D_1^2(\delta_2-h_2)^2-2D_1D_2(\delta_1-h_1)(\delta_2-h_2)+D_2^2(\delta_1-h_1)^2.$$

Obviously,

$$LHS \geq RHS.$$

Hence, (36) can never be satisfied, and (37) is the only choice, i.e.

$$\sqrt{\frac{D_1^2(\delta_2-h_2)+D_2^2(\delta_1-h_1)}{(D_1+D_2)}} \geq c \geq \frac{\mid D_1(h_2-\delta_2)-D_2(h_1-\delta_1)\mid}{\sqrt{(D_1+D_2)(\delta_1+\delta_2-h_1-h_2)}}.$$

□

Acknowledgments. The second author acknowledges support from the NSERC Discovery Grant RES0001528 and the FacSci Startup Fund RES0000381. We would like to thank Howie Weiss for proposing this work and providing some useful mathematical references when the second author was in Georgia Institute of Technology. Thanks to Mark Pollicott for the initial discussion.

REFERENCES

[1] S.Asei, B. Byers, A. Eng, N. James and J. Leto, "Bacterial Chemostat Model," 2007.

[2] P. K. Brazhnik and J. J Tyson, *On traveling wave solutions of fisher's equation in two spatial dimensions*, SIAM. J. Appl. Math., **60** (2000), 371–391.

[3] I. Chang, E. S. Gilbert, N. Eliashberg and J. D. Keasling, *A three-dimensional stochastic simulation of biofilm growth and transport-related factors that affect structure*, Micro. Bio., **149** (2003), 2859–2871.

[4] M. Fontes and D. Kaiser, *Myxococcus cells respond to elastic forces in their substances*, Proceedings of the National Academy of Sciences of the United States of America, **96** (1999), 8052–8057.

[5] H. Fujikawa and M. Matsushita, *Fractal growth of Bacillus subtilis on agar plates*, J. Phys. Soc. Jpn., **58** (1989), 3875–3878.

[6] H. Fujikawa and M. Matsushita, *Bacterial fractal growth in the concentration field of nutrient*, J. Phys. Soc. Jpn., **60** (1991), 88–94.

[7] M. E. Hibbing, C. Fuqua, M. R. Parsek and B. S. Peterson, *Bacterial competition: Surviving and thriving in the microbial jungle*, Nature Reviews Microbiology, **8** (2010), 15–25.
[8] D. P. Hzder, R. Hemmerbach and M. Lebert, *Gravity and the bacterial unicellular organisms*, Developmental and Cell Biology Series, **40** (2005).
[9] C. R. Kennedy and R. Aris, *Traveling waves in a simple population model involving growth and death*, Bull. of Math. Biol., **42** (1980), 397–429.
[10] E. Keller, *Mathematical aspects of bacterial chemotaxis*, Antibiotics and Chemotherapy, **19** (1974), 79–93.
[11] F. X. Kelly, K. J. Dapsis and D. Lauffenburger, *Effect of bacterial chemotaxis on dynamics of microbial competition*, Micro. Biol., **16** (1988), 115–131.
[12] E. Khain, L. M. Sander and A. M. Stein, *A model for glioma growth*, Research Article, **11** (2005), 53–57.
[13] S. M. Krone, R. Lu, R. Fox, H. Suzuki and E. M. Top, *Modelling the spatial dynamics of plasmid transfer and persistence*, Micro. Biol., **153** (2007), 2803–2816.
[14] D. Lauffenburger, R. Aris and K. H. Keller, *Effects of random motility on growth of bacterial populations*, Micro. Ecol., **7** (1981), 207–227.
[15] D. Lauffenburger, R. Aris and K. H. Keller, *Effects of cell motility and chemotaxis on growth of bacterial populations*, Biophys. J., **40** (1982), 209–219.
[16] D. Lauffenburger and P. Calcagno, *Competition between two microbial populations in a non-mixed environment: Effect of cell random motility*, Bio. Tech. and Bio. Eng., **xxv** (1983), 2103–2125.
[17] M. Matsushita, J. Wakitaa, H. Itoha, K. Watanabea, T. Araia, T. Matsuyamab, H. Sakaguchic and M. Mimurad, *Formation of colony patterns by a bacterial cell population*, Physica A: Statistical Mechanics and Its Applications, **274** (1999), 190–199.
[18] M. Matsushita, F. Hiramatsu, N. Kobayashi, T. Ozawa, Y. Yamazaki and T. Matsuyama, *Colony formation in bacteria: Experiments and modeling*, Biofilms, **1** (2004), 305–317.
[19] M. Mimura, H. Sakaguchi and M. Matsushita, *Reaction-diffusion modeling of bacterial colony patterns*, Physica. A. Stat. Mech. Appl., **282** (2000), 283–303.
[20] J. D. Murray, "Murray JD," 1^{st}, 3^{rd} edition, USA, 2002.
[21] K. Nowaczyk, A. Juszczak A and F. Domka, *Microbiological oxidation of the waste ferrous sulphate*, Polish Journal of Environmental Studies, **6** (1999), 409–416.
[22] C. S. Patlak, *Random walk with persistence and external bias*, Bull. Math. Biophys., **15** (1953), 311–338.
[23] P. T. Saunders and M. J. Bazin, *On the stability of food chains*, J. Theor. Biol., **52** (1975), 121–142.
[24] R. N. D. Shepard and D. Y. Sumner, *Undirected motility of filamentous cyanobacteria produces reticulate mats*, Geobiology, **8** (2010), 179–190.
[25] J. M. Skerker and H. C. Berger, *Direct observation of extension and retraction of type IV pili*, PNAS, **98** (2001), 6901–6904.
[26] L. Simonsen, *Dynamics of plasmid transfer on surfaces*, J. General Microbiology, **136** (1990), 1001–1007.
[27] R. Tokita, T. Katoh, Y. Maeda, J. I. Wakita, M. Sano, T. Matsuyama and M. Matsushita, *Pattern formation of bacterial colonies by Escherichia coli*, J. Phys. Soc. Jpn., **78** (2009), 074005 (6 pages).
[28] Y. Wei, X. Wang, J. Liu, L. Nememan, A. H. Singh, H. Howie and B. R. Levin, *The populatiion and evolutionary of bacteria in physically structured habitats: The adaptive virtues of motility*, PNAS, **108** (2011), 4047–4052.
[29] J. T. Wimpenny, "CRC Handbook of Laboratory Model Systems for Microbial Ecosystems," **2** 1998.
[30] P. Youderian, *Bacterial motility: Secretory secrets of gliding bacteria*, Current Biology, **8** (1998), 408–411.
[31] A. Ishihara, J. E. Segall, S. M. Block and H. L Berg, *Coordination of flagella on filgmentous cells of Escherichia Coli*, J. Bacteriology, **155** (1983), 228–237.
[32] B. L. Taylor and D. E. Koshlard, *Reversal of flafella rotation in Monotrichous and Peritrichous bacteria: Generation of changes in direction*, J. Bacteriology, **119** (1974), 640–642.

Received September 15, 2012; Accepted November 13, 2012.

E-mail address: silogini@math.ualberta.ca;silojude@hotmail.com
E-mail address: hao8@ualberta.ca